Abstract

WALKER, MATTHEW JAMES. Fabrication of a Graphitic Layer for Nanotribological Studies of Temperature Rise in a Frictional Contact Area. (Under the supervision of Professor Jacqueline Krim.)

In this thesis I use a quartz crystal microbalance (QCM) to investigate the interfacial heat rise of an adsorbed Kr layer on a single layer of graphite called graphene. The graphene surface is made by reacting CO to a 1000 Å thick Ni(111) surface at a temperature of 400 ºC. A 100 Å Ti layer is the base layer the Ni is deposited onto. The surface is characterized using Auger electron spectroscopy (AES) under ultra high vacuum conditions. The change in frequency vs. pressure/coverage graphs on a linear scale shows at what pressures a monolayer of Kr forms. The frequency vs. pressure/coverage graphs on a log scale show phase changes that can be compared to well known static phase changes. The comparison of the static phase change to the dynamic phase change yields an inferred temperature at the interface. This inferred temperature remained the same regardless of the sliding velocity. The latter observation, which is one principal point of this thesis, remains true irrespective of surface quality.

FABRICATION OF A GRAPHITIC LAYER FOR NANOTRIBOLOGICAL STUDIES OF TEMPERATURE RISE IN A FRICTIONAL CONTACT AREA

by
Matthew J. Walker

A thesis submitted to the Graduate Faculty of
North Carolina State University
in partial fulfillment of the
requirements for the Degree of
Master of Science

PHYSICS

Raleigh
2005

APPROVED BY:

Dr. Thomas Pearl Physics	**Dr. Harald Ade** Physics
Dr. Jacqueline Krim Physics Chair of Advisory Committee	

BIOGRAPHY

I was born in New Castle, Pennsylvania in March of 1978. I lived most of my years in southeast Michigan where I graduated high school from Airport High in 1996. In December 2001 I received my bachelor's degree in Engineering Physics, Computer Aided Design and a minor in Math from Eastern Michigan University.

TABLE OF CONTENTS

LIST OF FIGURES

Chapter 1: Introduction

1.1 Motivation

It is estimated that $420 billion or 6% of the gross national product of the US is lost to friction and wear [1]. It can be argued that all friction can be reduced to the atomic scale. The nanotechnological revolution has made fundamental atomic friction laws, that are currently being explored all the more important because the frictional forces are relatively larger forces in these microscopic systems than their macroscopic counter parts. Examples of such devices are hard drives in computers, miniature motors and RF micro-electro-mechanical system (MEMS) switches in satellites. All of these devices have sliding components subject to significant frictional forces that cause heating at the interface. The heating can cause the surface to chemically react or melt contact points which in turn can cause premature failure of a device [2]. Simulations trying to quantify the amount of heating sliding surfaces produce via friction differ by orders of magnitude [1, 3]. This thesis is a study of friction induced heating, i.e. tribo-induced heating, of a sliding Kr/graphene interface on a quartz crystal microbalance (QCM).

The type of friction causing the interface to increase in temperature is phononic in nature. Phononic friction was first suggested by Tomlinson in 1929 [4]. His model has two surfaces slipping across each other at a wear-free interface so that the only frictional force contribution can come from the vibrational modes of the atomic lattice. Tabor and Israelachvili in the 1970's used a surface force apparatus (SFA) to show the first experimental evidence of atomic scale friction in the absence of wear [5], a result consistent with phononic friction. The SFA has two mica surfaces that are atomically flat with a

lubricant between them. The normal and frictional forces can be measured for any given lubricant between the two mica faces.

In the late 1970's and early 1980's phononic friction was revisited, independently from Tomlinson's work. Lateral force microscopy (LFM) or often called atomic force microscopy (AFM) was used to measure atomic scale friction [6], seeking to detect phononic friction. An AFM uses a pointed tip that is dragged across a substrate. The angular deflection of the tip is detected by a laser reflected off the cantilever holding the tip and into a four quadrant photodiode. The scanning speeds of the AFM are ~1 micron/second and the tip of the AFM is usually a Si based material. Neither AFM nor SFA has to date detected the presence phononic friction in a definitive manner.

This thesis examines the sliding friction of Kr gas condensing onto a QCM substrate. A QCM, discussed in more detail in chapter 2, is a crystalline SiO_2 substrate that can oscillate a metal electrode at a stable frequency and amplitude. For a QCM, the sliding speeds are on the order of a centimeter per second and measure the average friction over a larger surface area then an AFM. Since the time scales for a QCM are faster than an AFM, therefore closer to the phonon lifetime, a QCM can measure phononic friction more accurately.

1.2 Past Computational Work

As mentioned above, phononic friction is the sliding induced excitation of atomic lattice vibrations. In 1997, Tomassone et al. employed two methods to measure the frictional forces and only considered phononic friction as the source of energy dissipation. The simulation consisted of an adsorbed Xe film on a Ag substrate and compared them to the

frictional results of Daly and Krim who investigated Xe on Ag with a QCM [1, 3, 7-10]. Method one of Tomassone et al. applies an external force on the adsorbate at time $t<0$ that causes the adsorbate to slide across the Ag substrate. Usually a thermostat is used to add or remove energy to the system to maintain a constant temperature throughout the system during the experiment. This adding or removing energy excites or damps the adsorbate film. Any damping from the thermostat would introduce an additional frictional force at the interface of the Xe and Ag. This is not desired because the only frictional force being considered is phononic friction. Therefore when the external force is pushing the adsorbate at $t<0$ the thermostat will measure the temperature and when the system is in equilibrium the external force and thermostat will be removed. This allows for only phononic friction to slow the adsorbate. The highest temperature rise observed by Tomassone was 13 K and occurs for the largest value for the initial velocities.

Method two simulated a QCM experiment by having no external force acting on the adsorbate. The QCM simulation is described by a linear response of the frequency and the substrate velocity as adsorbates are added to the film. The response defines the acoustic impedance and relates it to the friction. There were no interface temperature measurements for this method.

All methods match well with Daly and Krim's friction results. Method one has an initial discrepancy which is thought to be from the heating at $t<0$. Regardless the methods took into account phononic friction only. However, given uncertainties in what is known about the Ag(111) substrate corrugation, electronic effects could not be ruled out entirely. This is not an issue for graphitic substrates, where the substrate potentials are extremely well characterized.

1.3 Tribo-Induced Heating and Monolayer Melting On Graphite

Graphite is a widely used substrate in both experimental and computational surface science because the surface is covalently closed and the lamellae have weak interactions with each other. Therefore, the surface of graphite will not react with different species in an ultra high vacuum (UHV) system and the top lamellae layer can be modeled as the only surface interaction with an adsorbate layer. A well known adsorbate on graphite, both experimentally and theoretically, is krypton. In the early 1960's, adsorption volumetry was the only way to study adsorption of gases on solids. Adsorption volumetry measures the amount of adsorbate on a substrate, the pressure of the 3D gas and the equilibrium temperature. This is achieved by having a large substrate in a set volume. A known amount of gas is let into the volume and the pressure is measured. The pressure difference of what should be measured and the value actually measured is converted to the amount of adsorbate on the surface of the substrate. The method has been applied at widely varying temperatures for various substrate-adsorbate combinations. Kr phase diagrams (figure 1.1) on exfoliated graphite have been well documented in the literature [11, 12]. The phase diagram is so well documented that the temperature of Kr and the two dimensional phases between gas, liquid, solid, commensurate and incommensurate are known for sub-monolayer coverages.

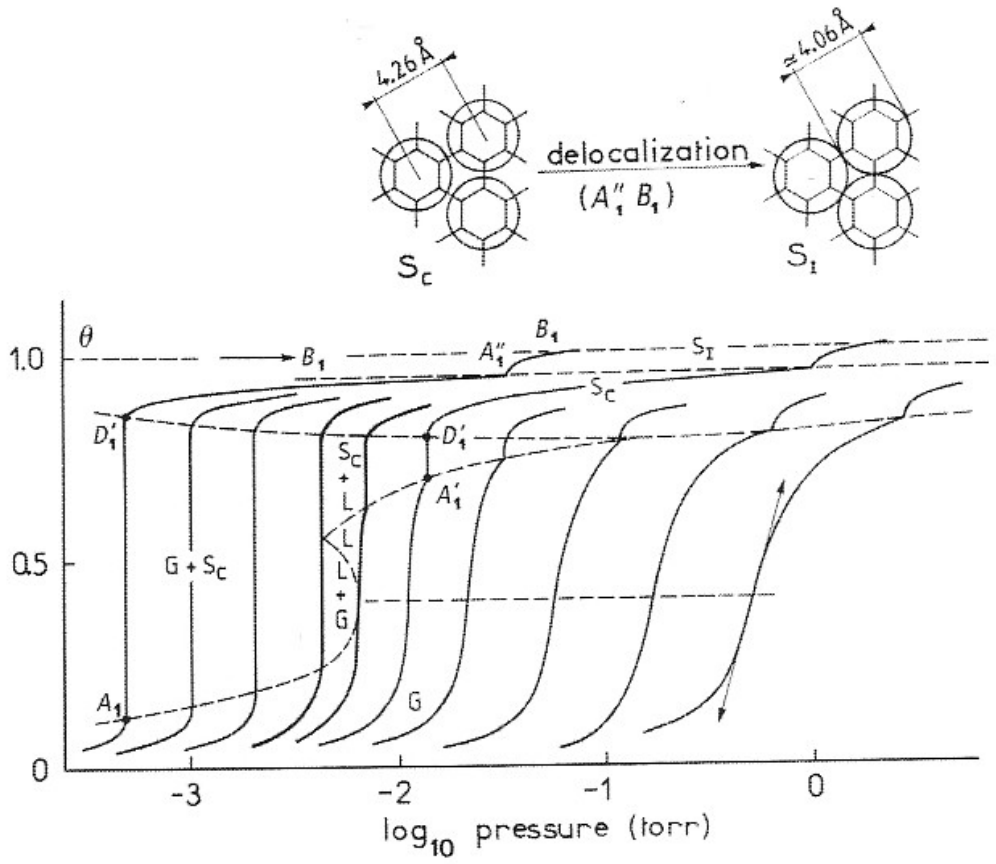

Figure 1.1. Volumetric adsorption isotherms of Kr/graphite at 77.3, 79.8, 82.3, 84.8, 86.0, 88.0, 91.8, 96.6, 102.6 and 109.5 K [11, 12].

The observations of step like features in the 2D physisorbed film are first order phase changes analogous to the physical phase changes in 3D bulk inert molecules. The 3D bulk molecules can exist in gas, liquid, or solid form depending on the temperature, pressure and density, $\rho = f(p,T)$. This is also known as the equation of state. 2D inert molecules can also exhibit these gas, liquid or solid changes depending on temperature, pressure and density, but at offset values. The 2D phase diagram changes because of the lack of nearest neighbors compared to the 3D phase diagram. The lack of nearest neighbors in the 2D films lowers the critical point and triple point [13]. The change in the 2D phase is not a uniformly compressed version of the 3D phase. The surface that the film is adsorbed on plays a bigger

role in the phase of the 2D adsorbed adatoms than the 3D bulk atoms. As the initial Kr monolayer is adsorbed, the 2D gas is compressed by the increase in pressure onto the surface and forms liquid and solid phases as additional layers are formed with increasing vapor pressure.

The experiment to follow uses a QCM, which I will describe briefly here, and more extensively in chapter 2. Since adhesives can not be used in UHV to adhere graphite to the QCM, a deposited metal electrode made in-situ has to be reacted to make a graphitic top substrate layer. In industry, it is common for a metal to react such that there is a monolayer of graphene, a single layer of graphite, on the surface. This process, sometimes unwanted in industry, is called poisoning or coking [14]. If the metal is not heated enough there will be no graphitic layer. This reaction is desired here but the heating of the piezoelectric QCM is limited because of its phase transition at 573ºC. So it is desirable to heat the sample enough to form a graphitic layer but not over heat the sample so it would not oscillate. Verification of the substrate surface is performed via Auger electron spectroscopy. Three metals have been found to possibly coke while staying below the phase transition of a QCM: nickel [14], iron [15], and cobalt [16]. It is well established that thermally evaporated FCC metals have mosaic oriented (111) surfaces [17]. Ni is one such metal. This experiment utilized a graphene layer synthesized on a Ni(111) electrode, made in situ with an electron beam evaporator, via a catalytic decomposition of CO shown in figure 1.2 [14].

$$2CO \rightarrow C + CO_2$$

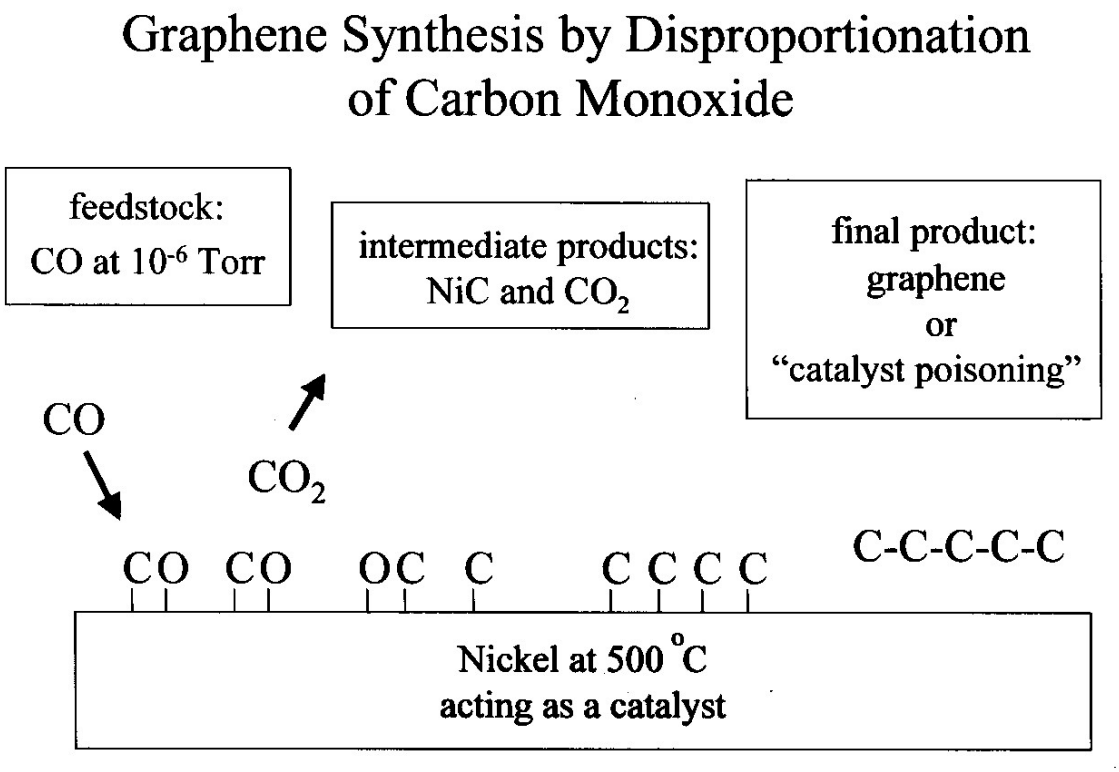

Figure 1.2. Reaction of graphene on top of nickel. [18]

Graphene commensurate on Ni(111) has a stretched lattice spacing of 2% compared to bulk graphite. The Kr phase diagram on stretched graphene may therefore vary slightly from that of graphite. This stretched lattice spacing and adsorbed Kr isotherm will be compared to the static phase diagram (figure 1.1) to infer a heating increase from the 77.4 K experimental cell. The heating dependence of the driving amplitude is also investigated by showing multiple vibrational amplitudes and how it effects the change in frequency isotherm.

1.4 Characterization of the Electrode

Characterization of the electrodes was performed with an Omicron Nanotechnology Multiprobe system [19]. The samples made in this thesis are transported to the Omicron system after the Kr isotherms and calibrations are done for surface analysis. Since a

graphitic substrate is inert most molecules adsorbed to the surface are physisorbed and not chemisorbed. These physisorbed molecules can be desorbed by heating the sample to 200ºC. To show that most of the adsorbed molecules are desorbed after baking in the Omicron system Auger spectra was taken for the initial samples before and after baking. Post-baked samples showed elements of the composed electrode plus oxygen. Oxygen is accounted for by assuming some amount will chemisorb to the Ti, Ni, and even Cu at varying degrees.

The percent of each element, φ, on the surface can be quantified by:

$$\varphi = \frac{\frac{I_e}{s_e}}{\sum_i \frac{I_i}{s_i}} \cdot 100$$

Where I_e is the intensity of the dominate peak of an element and s_e is the relative sensitivity factor for Auger. The denominator is the sum of all the elements in a spectrum. Included in the carbon peak is an indicator of how the carbon is bounded on the surface. Graphitic single crystal has a slight knee in the lineshape just before 270 eV and is shown in figure 1.3 [20]. Diamond AES has no such knee and is also shown in figure 1.3. In chapter 4 I show AES spectra with carbon peaks of different samples that have the graphite knee. The percentage of the carbon composition varies from 57.3% to 59.4%.

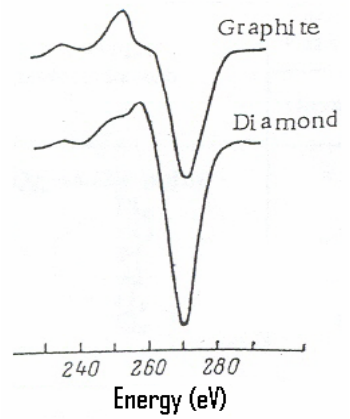

Figure 1.3. Auger of a carbon peak for graphite and diamond single crystal [20].

Chapter 2: Experimental Apparatus

2.1 Quartz Crystal Microbalance (QCM)

The QCM is a well established tool for monitoring real time adsorption of materials onto its surfaces [21]. The QCM is a piezoelectric made of crystalline SiO_2, oscillating in a shear mode, i.e. AT-cut, (Fig 2.1.) and has a solid-solid phase transition to a non-piezoelectric phase at 573ºC [22].

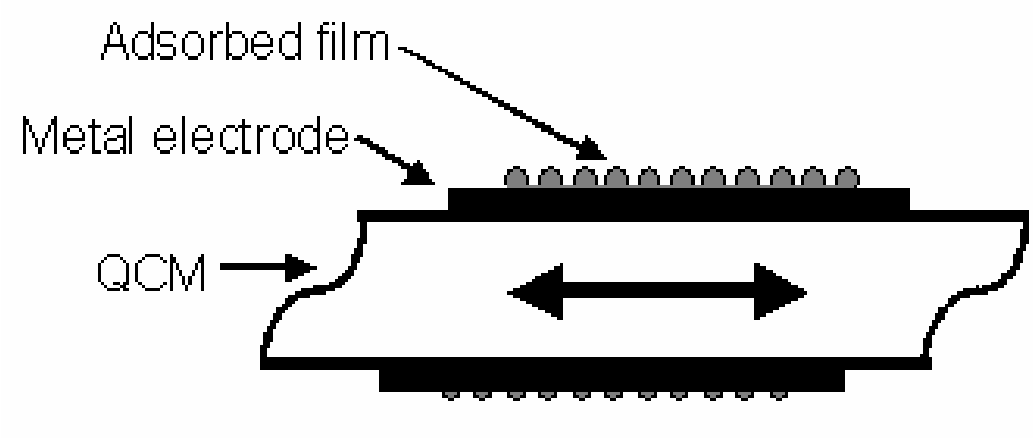

Figure 2.1. Side view of an AT-Cut QCM oscillating in transverse shear mode with electrodes and an adsorbate layer.

Since the QCM is a piezoelectric material applying an AC voltage close to its natural resonant frequency will result in oscillations with the proper feedback circuit. This frequency is determined by the crystalline orientation and thickness of the disk. Packaging of the QCM has three parts (Fig 2.2.): a quartz crystal [23], a quartz crystal mount that has two spring clips that attach to the QCM and a stainless steel custom made evaporation mask. The purpose of the evaporation mask is for the QCM to be protected from damage when

being moved to different evaporation areas and cryostat cell within the chamber and to pattern the electrode.

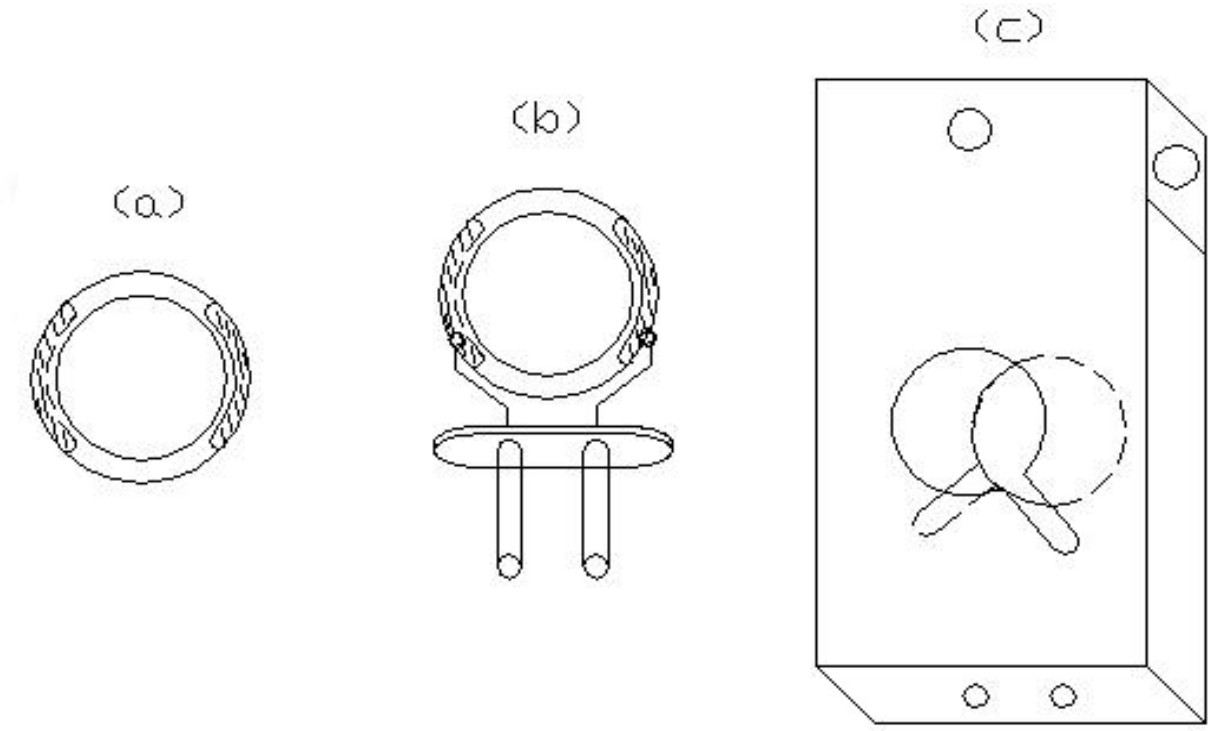

Figure 2.2. Components that make up the sample. (a) QCM with copper electrodes (b) QCM mounted (c) evaporation mask with no QCM inside

Figure 2.3 illustrates the Varian VT-112 ultra high vacuum (UHV) chamber with five 80 l/s ion pumps. Four pumping stages and a bake are used to achieve a base pressure of mid 10^{-10} Torr. Initially a sorption pump is used from atmosphere to reach 10^{-3} Torr range. From 10^{-3} Torr range a diffusion pump is used to pump to high vacuum, 10^{-7} Torr. When using the diffusion pump a liquid nitrogen trap on top of the diffusion pump is filled to protect from any back flow from either the diffusion or mechanical pump. At high vacuum five ion pumps are used to achieve an UHV pressure of mid 10^{-10} Torr. A titanium sublimation pump (TSP) is used to help pump residual H_2, O_2, N_2 and H_2O gases while using the ion pumps.

Baking is done while pumping with the diffusion and/or ion pumps. Baking the chamber for a period of time then turning the bake off speeds up the time it takes to achieve UHV conditions inside the chamber compared to not baking the chamber at all. Regardless of what pump is pumping, the system baking temperature is approximately 150 ºC to 200 ºC. Typically the pressure is in the lower 10^{-8} Torr to mid 10^{-8} Torr when the bake is turned off. Bake times last anywhere from overnight to three days depending on how much the system was exposed to atmosphere.

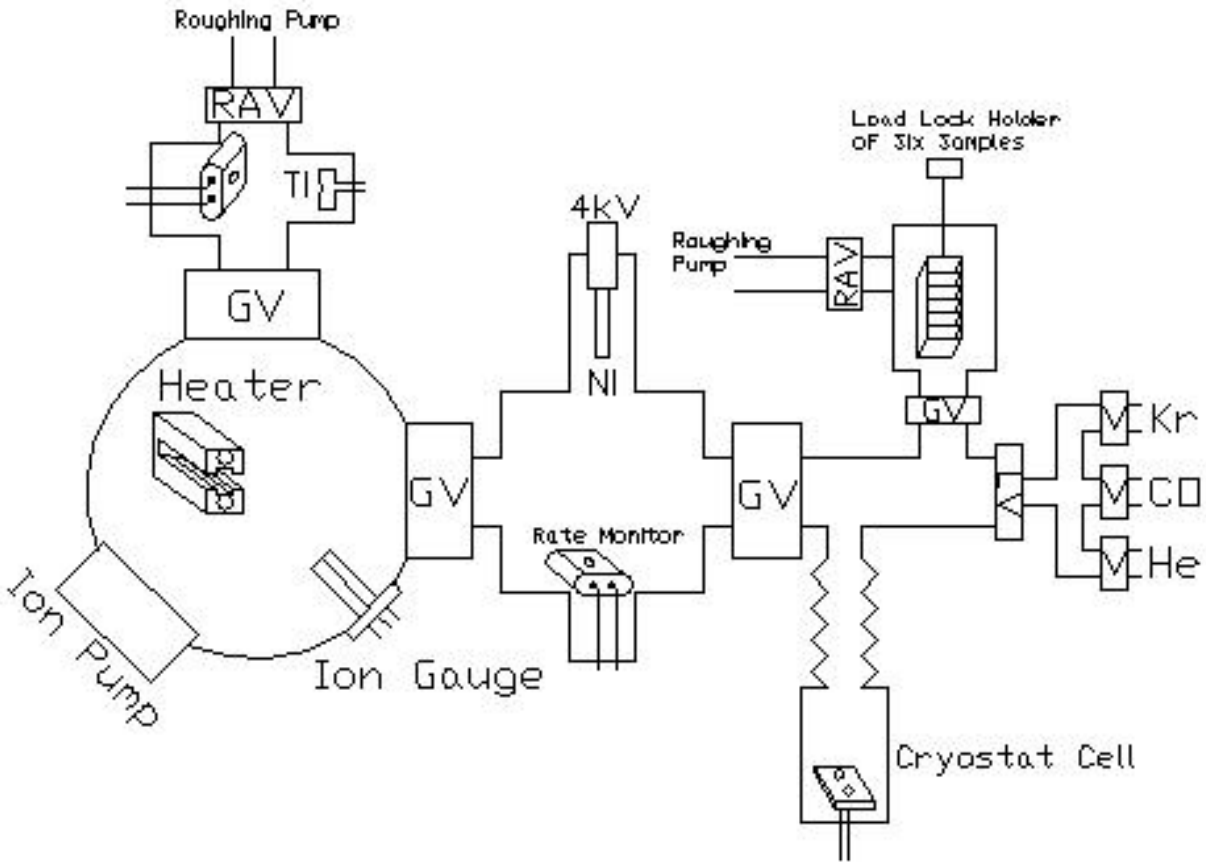

Figure 2.3. Schematic of the UHV chamber showing the gate valves (GV), right angle valves (RAV), leak valves (LV) and ¼" copper line valves (V) separating the system at different areas.

When depositing metals on an oscillating QCM, the frequency changes proportionally to the mass deposited onto the surface. Assuming a uniform deposited material is distributed across one face of the surface, the following equation can be used [21]:

$$\delta f = \frac{2 f^2 \rho d}{\rho_q v_q} \tag{2.1}$$

where ρ is the density of the deposited metals, d is the thickness of the metals, ρ_q is the quartz density and v_q is the speed of sound in quartz. For an AT-cut crystal ρ_q=3340 m/s and v_q=2650 Kg/m^3. When adsorbing gases onto both side of the QCM the change in frequency is:

$$\delta f = \frac{4 f^2 \rho d}{\rho_q v_q} \tag{2.2}$$

The factor of two from equation 2.1 to this equation is because the gas is adsorbing onto both sides of the crystal. When depositing materials on a QCM the amplitude changes and is related to the quality factor Q by [24]:

$$\delta\left(\frac{1}{Q}\right) = c\delta\left(\frac{1}{A}\right) \tag{2.3}$$

The proportionality constant, c, in this experiment is determined by performing a He isotherm. Since the He is a gas at 77 K the only damping is from the increasing pressure. The Q for the QCM used is around 10^5 and is defined as:

$$Q = 2\pi \frac{Mechanical\ Energy\ Stored\ Per\ Cycle}{Energy\ Lost\ Per\ Cycle} \tag{2.4}$$

The driving mechanism provides the stored energy and internal friction contributes to the energy lost, therefore the higher the Q the lower the loss and the higher the frequency stability. The driving mechanism used often in this lab is the pierce oscillation circuit, which

is described in more detail below. When the δQ and δf changes are known the slip time can be calculated by [21]:

$$\delta\left(\frac{1}{Q}\right) = 4\pi\,\tau(\delta f) \tag{2.5}$$

The slip time is a direct measure of how much slippage is at the adsorbate-substrate interface and is the time it takes for the QCM to reach 1/e when the oscillation is stopped.

2.2 Sample Preparation

In a separate chamber the QCM has a Cu tab 1000 Å thick deposited on both sides. These tabs are on the outer part of the disk and cover about a quarter of the circumference (Fig 2.2a.). The QCM is then placed in the spring clips, shown in figure 2.2b, in a right handed orientation so that when the electrodes are deposited they overlap a tab on either side of the QCM. Silver paint on the sprint clips is used to ensure an electrical connection and acts as a glue to hold the QCM in the spring clip. The QCM is mounted with a high temperature cement to attach it to the evaporation mask. This is then put into the main chamber where the experiment is performed.

2.3 Heating Stage

The main chamber houses a custom made stainless steel heater mounted on a vertical adjusting and rotating stage (Fig 2.3). A 0.030" W wire lined with ceramic beads runs through the top and bottom of the heater with a current typically around 19 A. The heating stage is used for two things:

- To initially outgas the new sample in the chamber, typically 200 ºC to 300 ºC with a current of 10 A.

- As a catalyst for nickel and CO to form a graphitic layer, 400 ºC with a current of approximately 19 A.

Because of the solid-solid phase transition of quartz at 573 ºC I need to be careful to not exceeding this temperature [22]. Over heating the QCM can cause the crystal to not oscillate, oscillate at spurious frequency responses or oscillate at overtones of its natural frequency. Therefore, the temperature is measured with a K-type thermocouple that is calibrated at a position 0.5cm away from the electrode face. A voltage of 14 mV, which corresponds to 345 ºC, is measure as the calibrated sample temperature of 400 ºC. After depositing nickel it takes about an hour to heat the sample to 400 ºC.

2.4 Additional Chambers

Off of the main chamber area are two areas where the samples can be moved through. These chambers are 90º from each other and have gate valves (GV) that isolate them from the main chamber. These GV allow for repairs while maintaining the main chamber at UHV conditions and save many hours of research time because baking the chamber is reduced. They also extend the ion pump lifetime because the ion pumps continually pump at lower pressures.

2.5 Ti Evaporation

The initial electrode is 100 Å of titanium. The reason for Ti is that Ti wets the quartz surface better than nickel and the Ni has a closer surface energy to Ti then quartz. This allows for a smoother Ni electrode. The Ti is deposited via thermal evaporation. The current through the molybdenum filament coated with Ti is between 38 A and 42 A, the pressure

during deposition ranges between the mid 10^{-9} Torr to low 10^{-8} Torr and the deposition rate ranges between 3 Hz/min to 6 Hz/min. A 5 MHz AT-cut rate monitor ordered from Crystek is used to measure the electrode thickness [25].

2.6 Ni Evaporation

Ni is the second layer of the electrode deposited via electron beam evaporation to 1000 Å to 1500 Å thick. Past experience in the Krim lab has shown thermal evaporation with a W boat does not work as well as thermal evaporation with an electron beam. The configuration for the e-beam is illustrated in figure 2.4. The Ni rod is suspended from an electrical feedthrough at a potential 4.1 kV. A coiled W wire is horizontally offset from the nickel and carries a current ranging from 4.5 A to 5.2 A. Electrons will emit from the W wire with energy of the electron charge, e, multiplied by the potential difference, V, and collide with the nickel rod. After the Ni rod has been heated enough Ni particles will evaporate from the rod. Some of these emitted particles will be deposited onto the sample and rate monitor placed below the rod. The pressure ranges between the mid to upper 10^{-9} Torr during deposition and the deposition rate ranges between 30 Hz/min and 60 Hz/min.

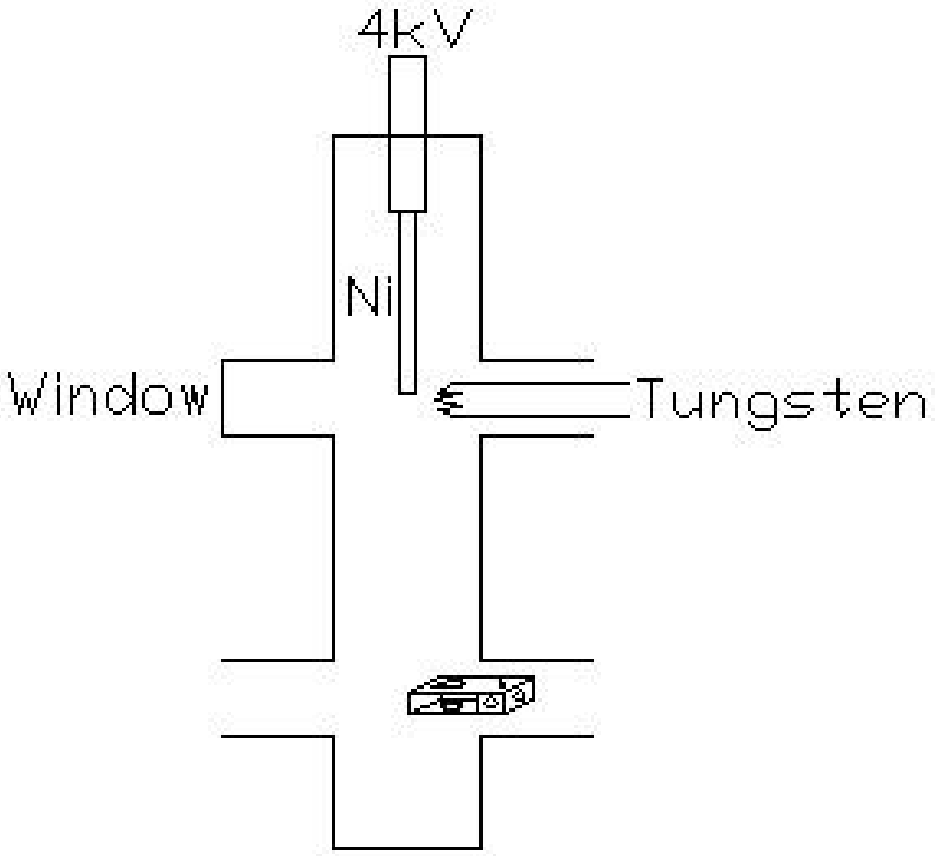

Figure 2.4. Electron beam evaporation area for Ni deposition.

2.7 Low Temperature Experimental Cell and Pierce Circuit

The low temperature experimental cell in figure 2.5 has two electrical feedthroughs so the sample can be connected to the pierce circuit in figure 2.6. After the sample is connected to the pierce circuit the cell is chilled to 77.4 K by submerging it into a dewar filled with liquid nitrogen. Outside the chamber is a second pierce circuit oscillating a QCM at a frequency difference less than 50 kHz from the QCM oscillating inside the chamber. The reason for this tolerance is because the Keithley 197A multimeter. The two signals from the pierce circuits are connected to a mixer that has a low pass filter. The output leads from the low pass filler connect to the Phillips PM6673 frequency counter and the Keithley 197A multimeter to measure the change in frequency, which is related to the mass of the absorbate,

and amplitude. The reason for using this mixed signal is for increased accuracy of the frequency. Over hours the frequency changes by one Hertz when the sample comes into equilibrium at liquid nitrogen temperatures.

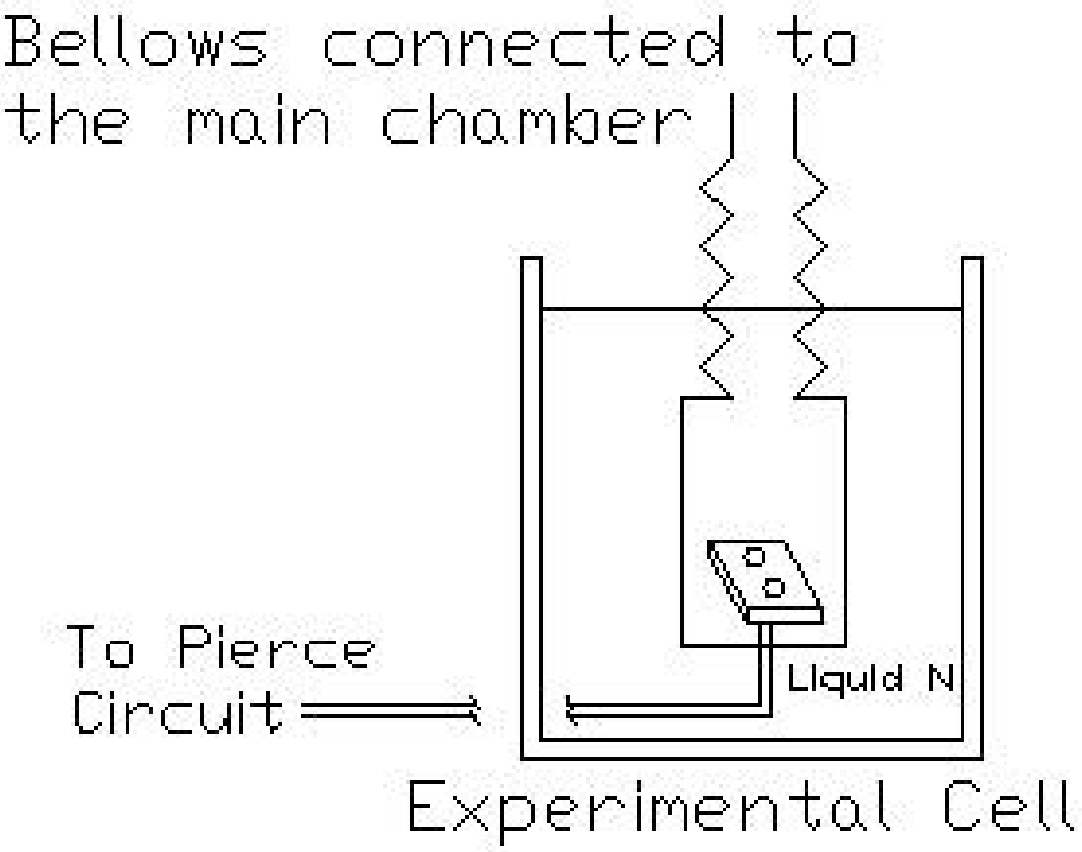

Figure 2.5. Experimental Cell submerged in liquid nitrogen and connected to a pierce circuit.

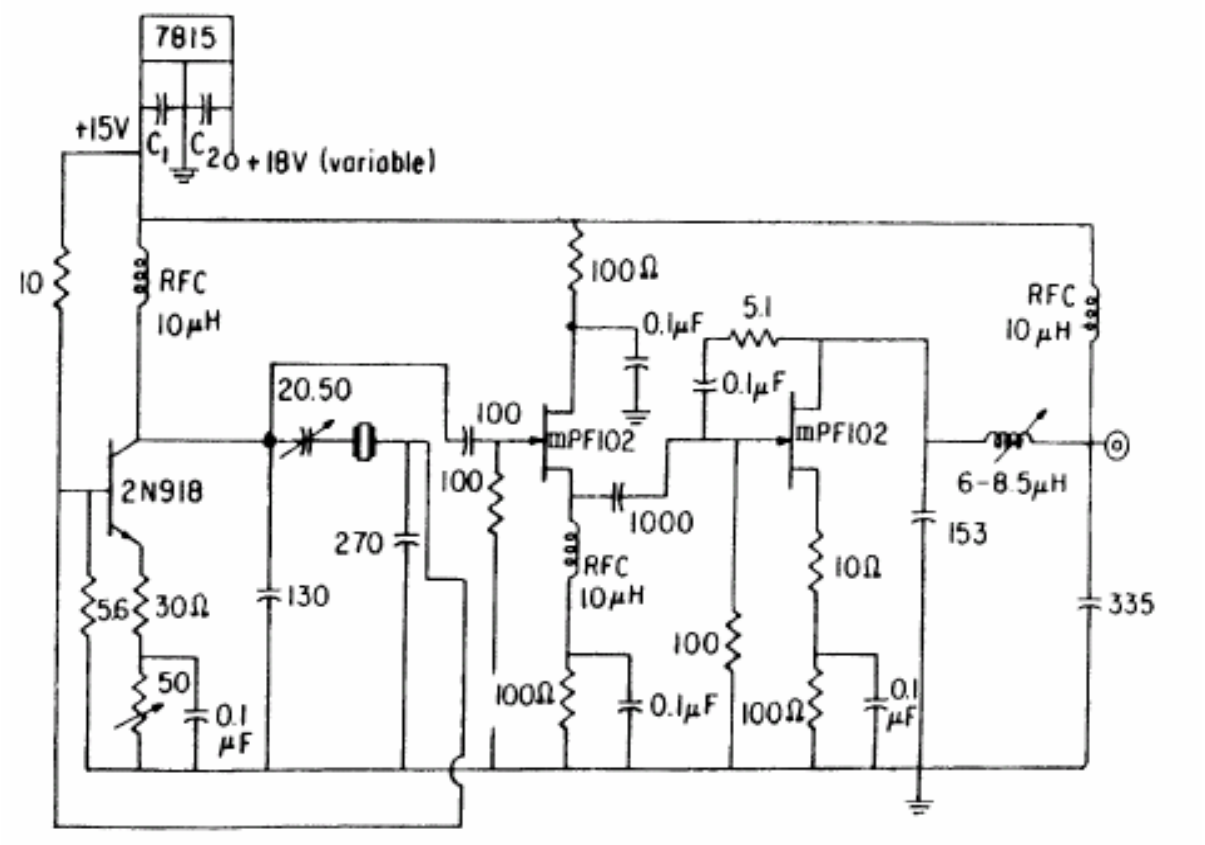

Figure 2.6. Schematic of Pierce Oscillator Circuit

2.8 Gas Dosing

At the end of this chamber is the gas dosing area. This area has three lines: one connected to CO for making graphene, one connected to Kr for the adsorb isotherms and one connected to He for the calibration isotherms. These lines are connected to the chamber by a leak valve so the flow of gas is controlled and therefore the pressure during a respective gas dosing is controlled. When the sample is baked to 400 ºC the leak valve is opened until the ion gauge reads in the mid 10^{-6} Torr. The sample is exposed to CO for 30 minutes. During the adsorb Kr isotherm the leak valve is opened to measure pressure ranging from $5x10^{-5}$ Torr to 1.8 Torr with the MKS PR4000 controller and two MKS 628 capacitance manometers an takes between 20 minutes to 30 minutes. These manometers have a combined pressure range

from $2x10^{-5}$ Torr to 100 Torr. These MKS manometers also measure the pressures, 10 Torr to 100 Torr, for my helium calibration isotherms. Previous experiments performed by my predecessors and then myself showed that when pumping the Kr gas out of the chamber the frequency change would change in a reverse path to the Kr gas being released into the chamber. When the release of the Kr gas is stopped the change in frequency will stay at a constant value. What is taken from this is that the rate at which the Kr gas is being release should not affect the shape of the frequency plots as long as the rates are at speeds the equipment can read. This also indicates that the samples are in equilibrium.

Chapter 3: Experimental Results

3.1 Introduction

This chapter describes the different electrode layers that make the substrates, under what conditions the substrates are made, documents the experimental results from the graphitic substrates and a progression of making better graphitic substrates. AES is implemented to characterization the substrates [19]. Change in frequency and amplitude versus pressure data are collected during each Kr isotherm. The change in frequency relates to the Kr monolayer formed on the QCM and is superimposed onto to the static phase diagram of Kr on graphite [11, 12] to infer the temperature of the interface.

3.2 Graphene On Ni/Cu/Ti Electrode

Early work for making an oscillating graphitic substrate had an initial oscillating electrode of Cu on Ti. This was done because making an all Ni oscillating electrode was proving difficult and it was assumed that the initial layer of the electrode would not migrate through the Ni when heated to 400 ºC to react the CO with the Ni to graphitize the top layer. With these early samples there were problems with making an oscillating electrode after baking the QCM because the heater was not well calibrated. It was concluded that I was baking the samples over the 573 ºC QCM phase transition. Doing isotherms on these samples was impossible since they didn't oscillate but some samples were taken to other systems for Auger. Isotherms and Auger spectra shown together are from samples that are made under the same conditions. Kr uptake on these samples is presented for comparison purposes only.

Starting from the QCM surface 100 Å of Ti is deposited followed by 800 Å Cu followed by 600 Å of Ni and finally the top surface of the Ni is reacted to CO, attempting to make graphene. The base pressure before depositing Ti is in the low 10^{-9} Torr and ranges between $3.8x10^{-8}$ Torr to $1.2x10^{-8}$ Torr while depositing electrodes at an average rate of 4.8 Hz/min. The Cu is deposited after the Ti at pressures ranging from $1.0x10^{-8}$ Torr to $8.2x10^{-9}$ Torr at an average rate of 120 Hz/min. After the Cu layers are deposited the sample is moved to the Ni deposition area. The pressure while depositing Ni ranges from $3.7x10^{-8}$ Torr to $2.0x10^{-8}$ Torr while depositing at an average rate of 20.0 Hz/min. The sample is then heated to approximately 400 ˚C which corresponds to a calibrated thermocouple temperature of 14 mV at a pressure of approximately $5.0x10^{-6}$ Torr for 30 minutes. The sample is then moved to the experimental cell and submerged into a liquid nitrogen dewar to perform the isotherms. The highest starting pressure for the Kr isotherm is the mid 10^{-8}Torr and is as low at $1.0x10^{-9}$ Torr for the first Kr isotherm. After all of the Kr isotherms and He calibrations the sample is removed from UHV and walked over in atmosphere to the surface analysis UHV system in our group. The sample is baked to approximately 200 ºC to desorb any physisorbed molecules when the sample was transported. Figure 3.1 shows the Auger spectra of a similarly made sample.

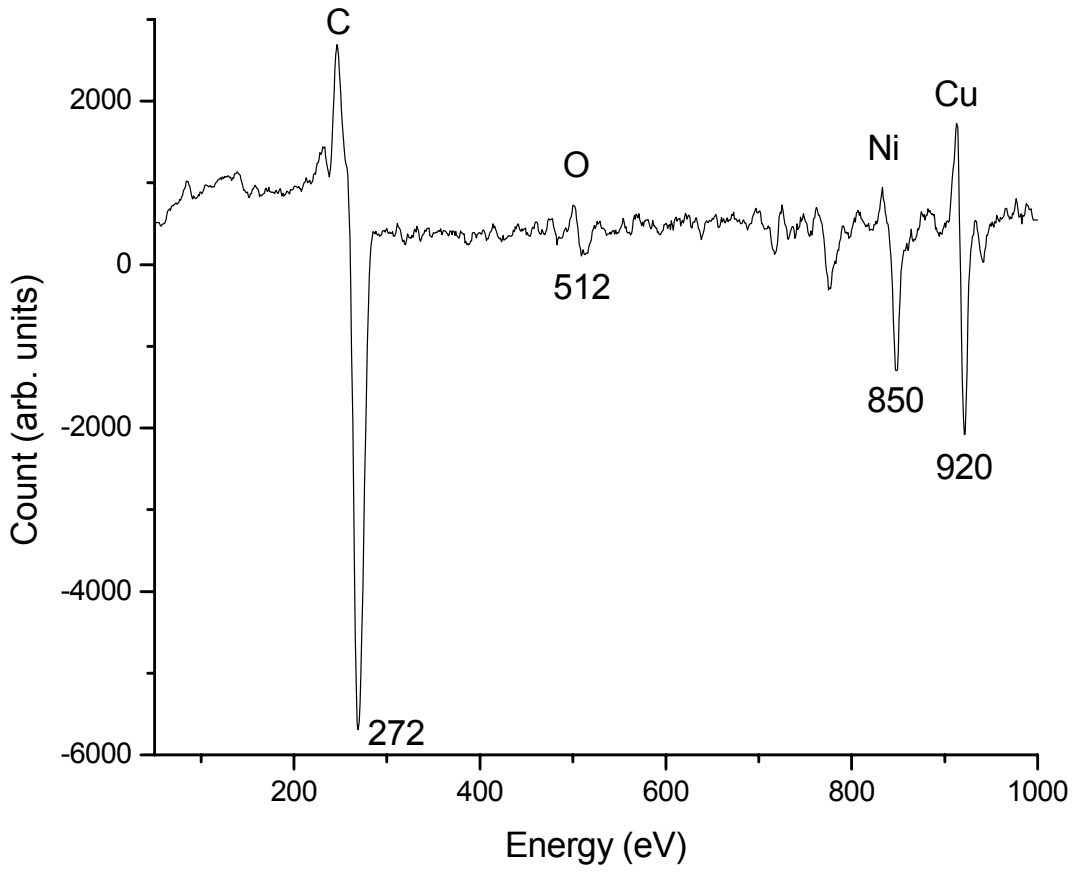

Figure 3.1. An Auger spectra of Ti/Cu/Ni/Graphene substrate

The Auger spectra show that there are four elements on the surface: 59.4% Carbon, 1.9% Oxygen, 12.7% Nickel and 26.0% Copper. The electrode is originally made so that the top layer is graphene on top of Ni on top of Cu on top of Ti. When heating the sample to react CO to the Ni to form graphene Cu must migrate through the Ni to the substrate surface or just a few atomic layers below the substrate surface. Both Ni and Cu oxidize so either or both can have had some oxygen bonded to them.

Figure 3.2 shows the change in frequency of the adsorption of Kr at three different starting amplitudes. The first knee in figure 3.2a is between 20 Hz to 25 Hz and corresponds

to the first monolayer. This is less than 26.6 Hz for an atomically flat graphitic substrate. The Cu migration has apparently altered the substrate so that a comparison can not be drawn to a graphite substrate.

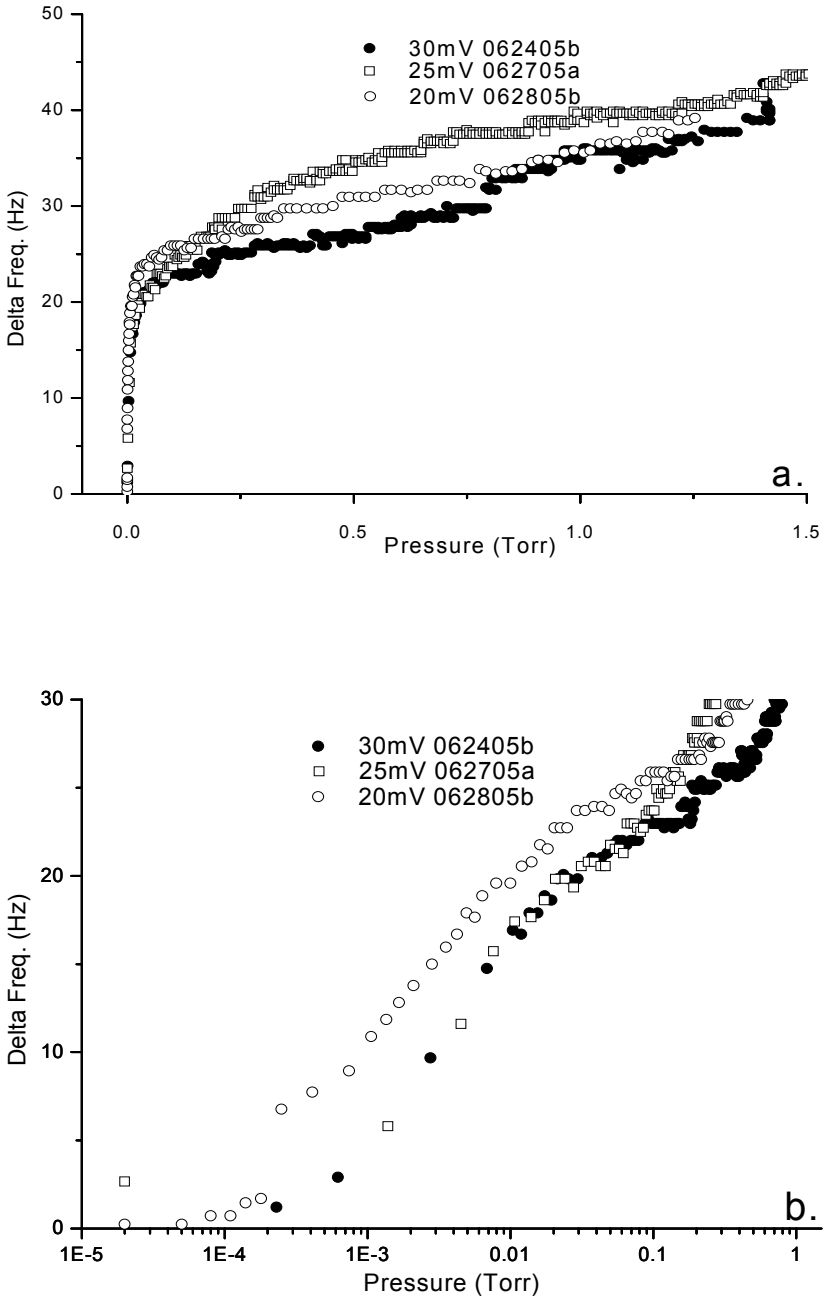

Figure 3.2. Changes in frequency as Kr is adsorbed onto a graphene substrate in linear (a) and log (b) graph. The initial amplitudes are measured from the pierce circuit with an oscilloscope in mV.

The steps in figure 3.2b are compared to figure1.1 to infer a temperature. Figure 3.3 shows the Kr isotherms from this thesis superimposed on the static Kr isotherms. It can be seen that there is no correlation between the two isotherms, which we attribute to the Cu migration changing the surface composition.

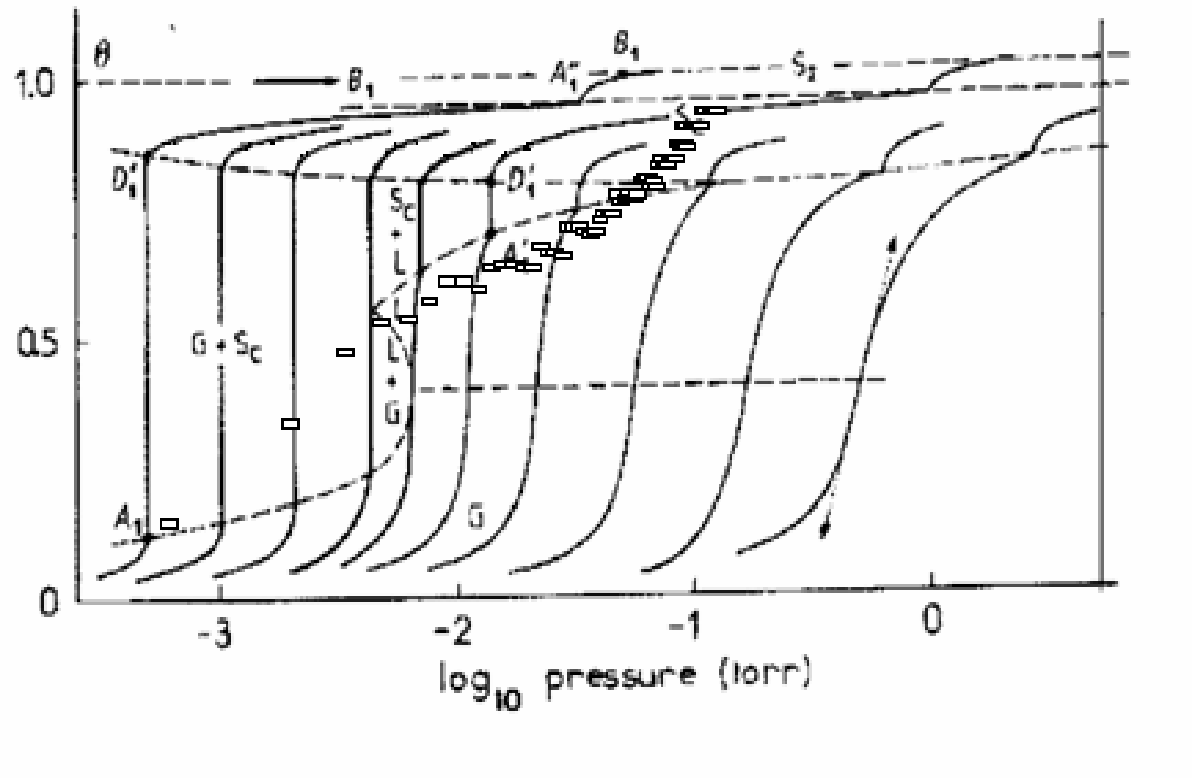

Figure 3.3 Kr isotherms at 25mV on a Ti/Cu/Ni/Graphene QCM superimposed on a static Kr Isotherm on graphite.

With these results we felt that the graphene layer was too contaminated with Cu to correlate the static Kr on graphite experiment. Therefore Cu was taken out and a Ti/Ni is made to get better results. The problem with this is that the QCM does not oscillate after depositing just Ti. Ti is used as a buffering layer to minimize the surface energy differences which helps to make a smoother surface. Cu was used to build up the electrode to get an

initial oscillating sample. This is a well established procedure in the Krim Lab. Ni deposition takes longer then Cu and there were no well defined layer thicknesses from previous experiments to go off.

3.3 Graphene On Ni/Ti Electrode

Starting from the QCM surface 100 Å of Ti is deposited followed by 1000 Å of Ni and then the top surface of the Ni is reacted with CO to make a graphene surface. The base pressure before depositing Ti is 1.6×10^{-9} Torr and ranges between 1.0×10^{-8} Torr to 7.4×10^{-9} Torr while depositing electrodes at an average rate of 10.0 Hz/min. After the Ti electrodes are deposited the sample is moved to the Ni deposition area. The pressure while depositing Ni ranges from 2.8×10^{-9} Torr to 4.0×10^{-9} Torr while depositing at an average rate of 35.0Hz/min. The sample is then heated to approximately 400 ˚C which corresponds to a calibrated thermocouple temperature of 14 mV at a pressure of approximately 5.0×10^{-6} Torr for 30 minutes. The sample is then moved to the experimental cell and submerged into a liquid nitrogen dewar to perform the isotherms. The highest starting pressure for the Kr isotherm is the mid 10^{-8} Torr and is as low at 1.0×10^{-9} Torr for the first Kr isotherm. After all of the Kr isotherms and He calibrations the sample is remove from UHV and walked over in atmosphere to the surface analysis UHV system [19]. The sample is baked to approximately 200 ºC, which corresponds to 0.4 A though the heater wires, to desorb any physisorb molecules when the sample was transported. Figure 3.4 shows the Auger spectra of the sample. Notice that this spectrum is a compilation of three smaller spectra taken consecutively. The reason for the compilation is because the original 100 eV to 1000 eV was lost and the sample is no longer around. In my lab book I have the original 100 eV to 1000 eV spectra and this compilation is an accurate reproduction of the original.

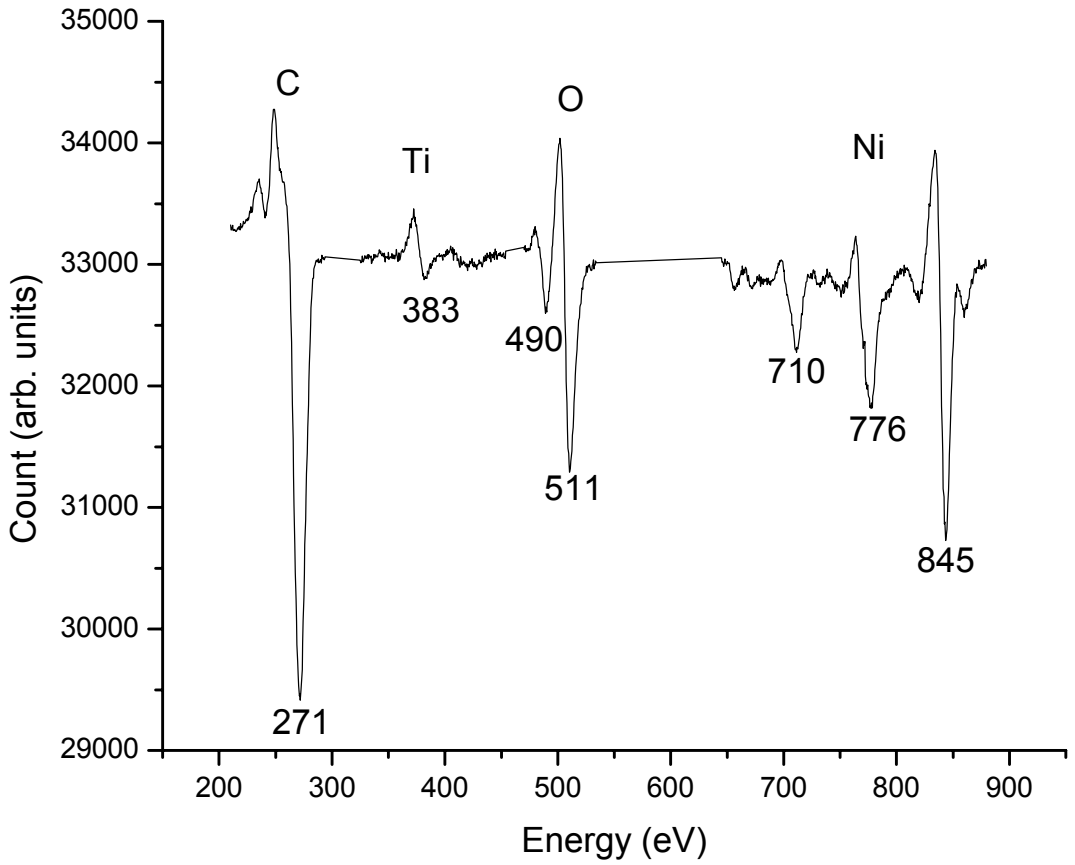

Figure 3.4. A compilation of three separate Auger spectra of a Ti/Ni/Graphene sample.

The Auger spectra show that there are four elements on the surface: 57.3% Carbon, 1.8% Titanium, 13.8% Oxygen and 27.1% Nickel. The electrode is originally made so that the Ni is 1000 Å below the graphene. When heating the sample to react CO to the Ni to form graphene Ti migrates through the Ni to the substrate surface or just a few atomic layers below the substrate surface. Ti is a fast oxidizer which is why TSP's are used in UHV as a getter pump. We believe Ti is forming TiO_2 with the CO, any residual oxygen in the chamber and/or the oxygen in atmosphere when the sample is transported to the Auger chamber. Therefore having a large oxide peak is not surprising. Since oxide is a

nonconductor it would also explain why imaging with STM is difficult. The Ni is not surprising because it is only one atomic layer below the graphene surface and Auger does penetrated that distance.

Figure 3.5 shows the change in frequency of the adsorption of Kr at five different starting amplitudes. The first knee in figure 3.5a are between 30 Hz to 35 Hz and correspond to the first monolayer. Using equation 2.2 I verified [26] that one commensurate monolayer of Kr on both sides of the QCM corresponds to a 26.6 Hz frequency shift and one incommensurate monolayer of Kr on both sides of the QCM corresponds to 27.9 Hz frequency shift. This shows that the sample is not strictly flat but it is as smooth or smoother then comparable experiments [18].

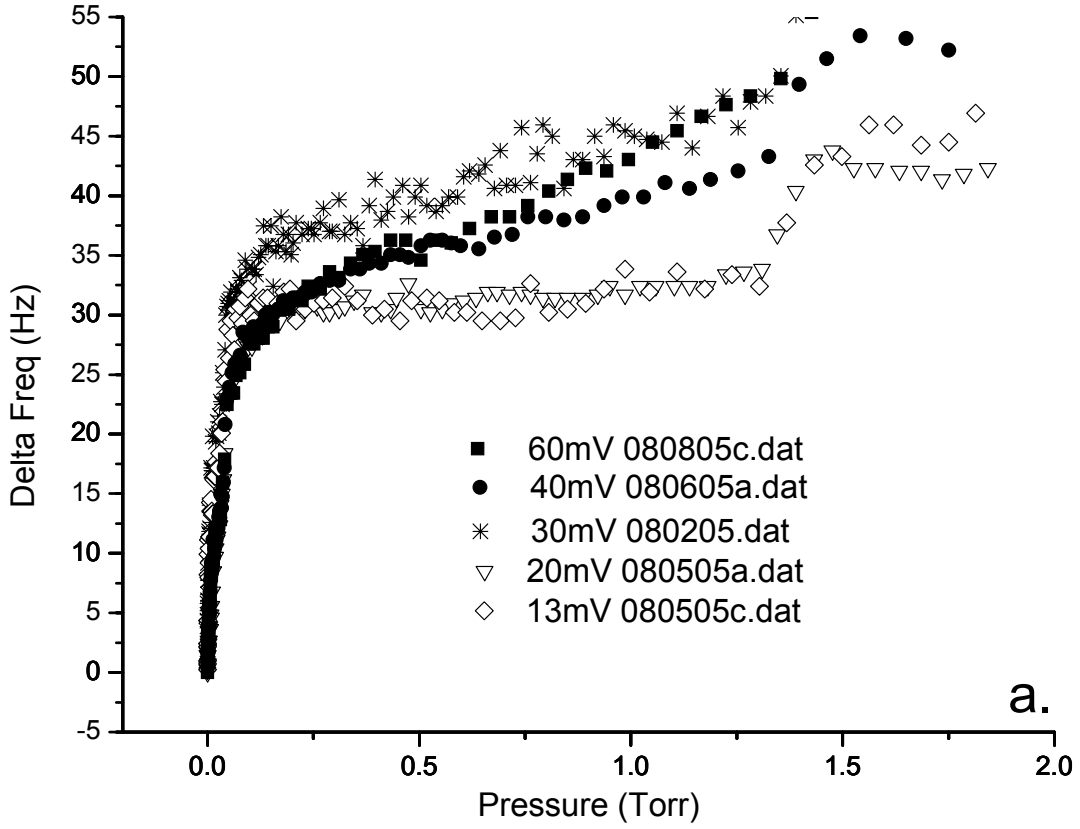

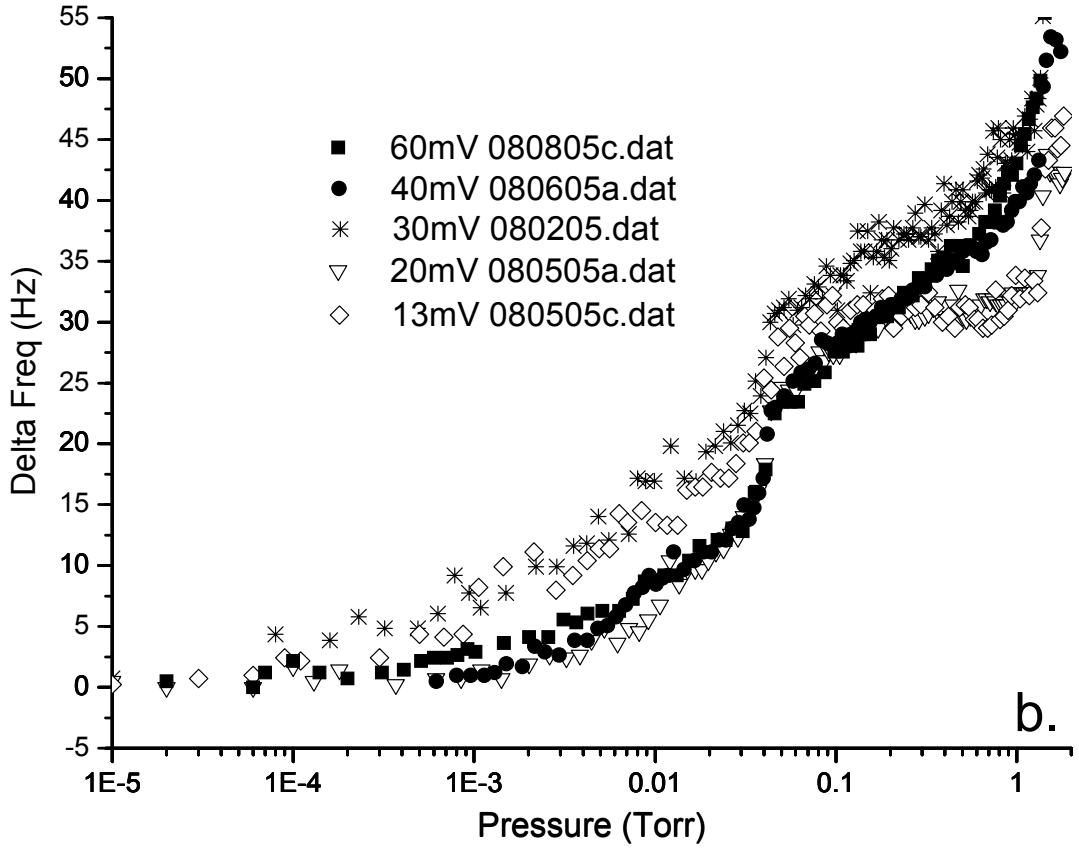

Figure 3.5. Changes in frequency as Kr is adsorbed onto a graphene substrate in linear (a) and log (b) graph. The initial amplitudes are measured from the pierce circuit with an oscilloscope in mV.

A step in figure 3.5b is superimposed onto figure 1.1 to infer a temperature (figure 3.6). Looking at figure 3.6 the QCM data falls between the static Kr isotherms of 88.0 K and 96.6K. This is approximately a 15.0 K ±5 K increase at the interface from the 77.4 K liquid nitrogen experimental cell. As the amplitude of the QCM changes the inflection point in the steps for the submonolayer remains the same. For the bilayers the change in frequency increases with increasing amplitude. This is explained by the fact that there is more cooling for increased Kr pressure. A rule of thumb is that for every 100 Hz change in frequency corresponds to 1 K increase of the sample when there are heating effects. At 1torr in figure

3.5b there is approximately 12 Hz difference between the 13 mV amplitude and the 60 mV amplitude data. This frequency shift corresponds to a 0.12 K increase in temperature from the smallest amplitude to the largest amplitude. The submonolayer phase diagram has at best 3 K resolution with the MKS Baratron capacitance manometers so the 0.12 K can not be resolved with the manometer.

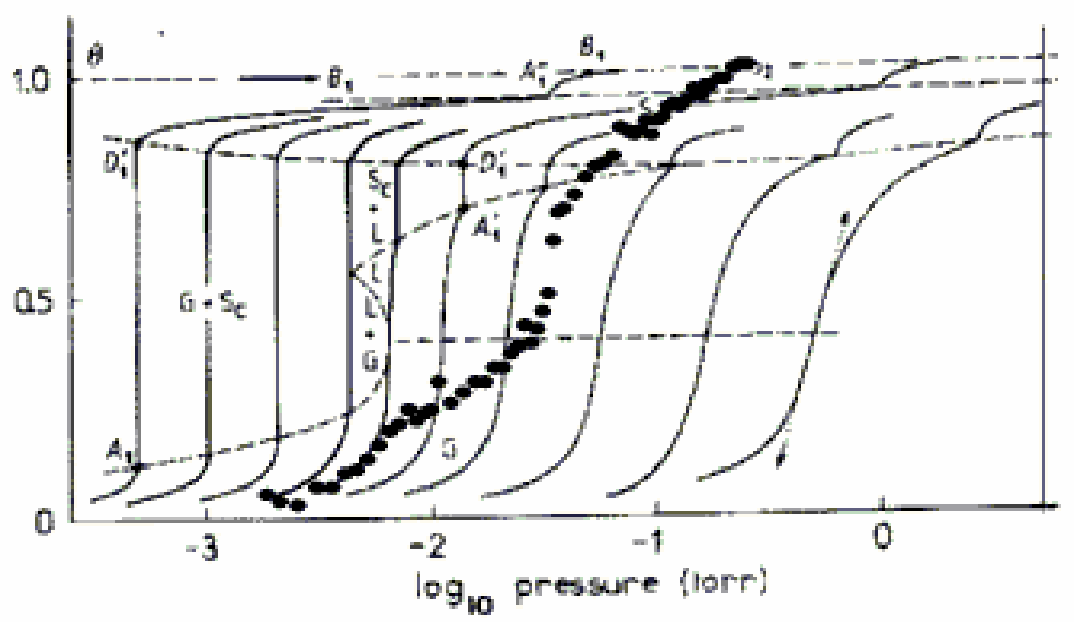

Figure 3.6 Kr isotherms at 60mV on a Ti/Ni/Graphene QCM superimposed on a static Kr Isotherm on graphite.

When taking the data the order of the amplitudes is not taking in ascending or descending order. This was to show that the sample was not being contaminated between Kr isotherms and He calibrations.

Figure 3.7 is the inverse amplitude data taken with the Keithley multimeter during the experiment. The simulation articles talked about in chapter one estimated the QCM velocity to be 1 cm/s to 2 cm/s which are common in the literature. Using a scanning tunneling microscope the velocity of the QCM has been measured for different amplitudes [27]. The

amplitudes in figure 3.2 converts to electrode velocities of 3.4 cm/s, 5.3 cm/s, 7.9 cm/s,10.6 cm/s and 15.8 cm/s with respect to 13 mV, 20 mV, 30 mV, 40 mV and 60 mV oscillating amplitude [28]. The adsorbed film velocities are 0.1 of the electrode velocities. These velocities are not to imply that if you extrapolate to 0 cm/s that you would have this heating still. At 0 cm/s the temperature should be 77.4 K because this in no heating from friction. The slowest electrode velocity is the lower limit of the experiment. The faster electrode velocity is not the fastest possible electrode velocity but it was unclear how fast to drive the electrode. So the velocities of this thesis and under the limitations of the equipment used, the heating at the interface do not change.

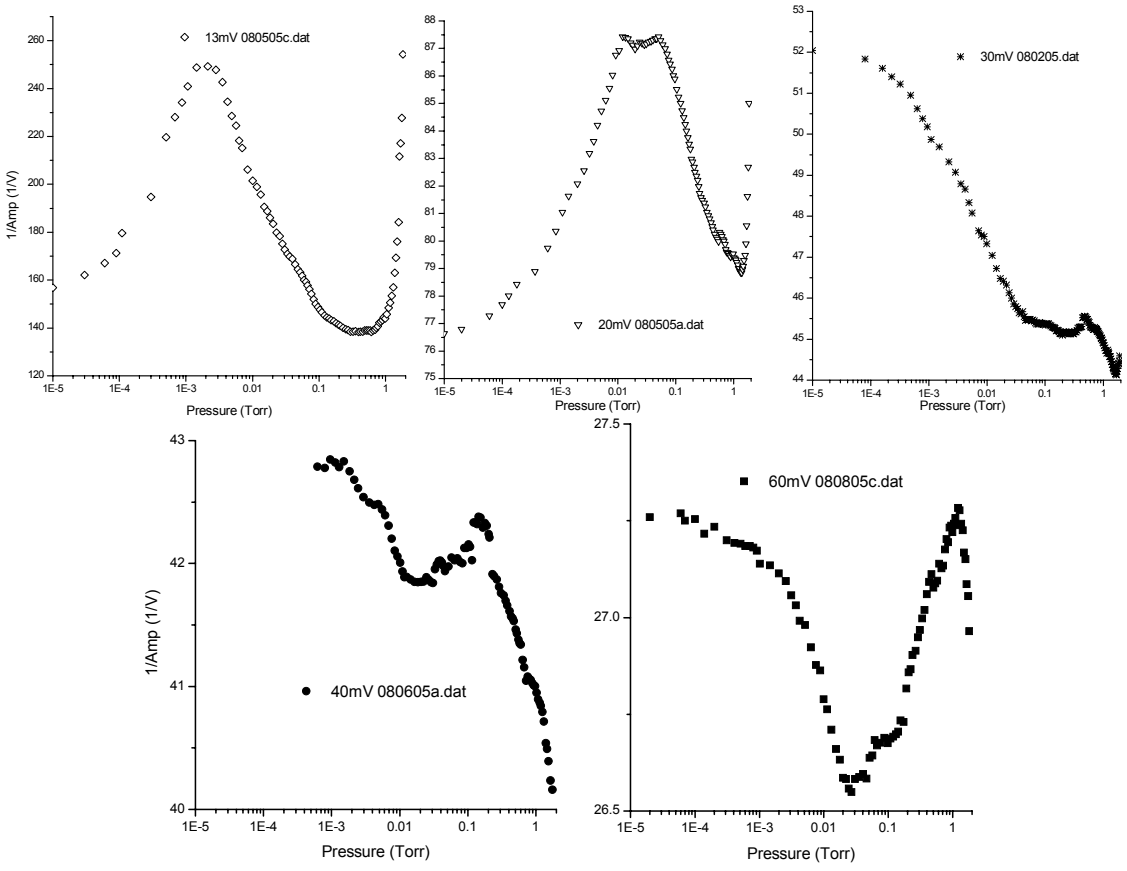

Figure 3.7 Changes in inverse amplitude as Kr is adsorbed onto the surface of the QCM.

Finally as the Kr isotherm reaches 1.5 Torr there is no more uptake on the electrode and the frequency doesn't changes. This is because the Kr is at its saturation pressure. At this point the Kr gas is condensing into a liquid at the coldest area of the experimental cell which is the walls. The sample can not be the coldest area of the experimental cell because as explained above the sample is self heating because of the oscillating velocities.

Chapter 4: Conclusion

4.1 Final Thoughts and Future Work

The Kr isotherm shown earlier on a Ti/Ni/graphene electrode has show an inferred increase in temperature of 15 K ±5 K. This temperature increase is constant with respect to sliding velocities for a submonolayer of Kr. Bilayers of Kr show self heating of the QCM of 0.12 K at 1torr between amplitude of 13 mV and 60 mV which corresponds to 3.4 cm/s and 15.8 cm/s. The electrodes are deposited under UHV conditions and the reaction to catalyze graphene is made in high vacuum. Kr and He isotherms are performed in an experimental sample cell submerged in liquid nitrogen. For every Kr isotherm there is a He isotherm that calibrates the QCM oscillations to a quality factor Q and a slip time. Surface characterizations are performed in a separate UHV chamber [24] therefore the sample has to be taken out of UHV and into atmosphere for a period of time. Since the sample has a graphene top layer most contamination from the transfer between UHV systems is physisorbed. The contamination can be removed by heating the sample to approximately 200 ºC. The Auger spectra show Ti migration to the top layers of the electrode. Oxygen is introduced to the surface at some undetermined time.

It was shown in earlier work that the Ti/Cu/Ni/Graphene electrode had too much Cu migration. The Kr isotherm data and comparison to static Kr on graphite data gave us reason to conclude that the Cu was changing the surface composition so much that there could not be any comparison made to infer a heat rise with the static isotherms.

Future work would include making an electrode with Ni and graphene only. The Ti had migrated thought the Ni, most likely during the heating of the sample to make graphene. This Ti that migrated to the surface is where we think a large amount of oxygen seen in the

Auger spectrum is bonding. The trade off to not using Ti may make the surface roughness increase because of a larger surface energy difference between quartz and Ni. Currently these samples have been very difficult to image with a STM. Oxidation is thought to be a factor preventing STM imaging. Removing the oxygen will hopefully make imaging possible. Finally it has been reported that depositing one monolayer of gold onto a graphene/Ni electrode will change the graphene stretched lattice spacing to bulk graphite spacing [29]. The monolayer of gold migrates through the graphene and resides on top of the Ni(111). Gold doesn't have the corrugated surface that Ni(111) has and allows the carbon atoms to relax into their natural spacing. Making a tunable substrate would be of great interest in helping to explain friction and thereby explaining heating at the interface. It will be interesting to see how the Kr isotherms differ between graphene substrates that are made on different under layers. This thesis had a Ni under layer for graphene but Fe and Co is thought to be compatible under the QCM temperature restrictions. Since Fe and Co a have different lattice spacing from Ni this possible tunability heating dependence would be interesting to investigate.

References

(1) B.N.J. Persson, Surf. Sci. **33**, 83 (1999); B.N.J. Persson, *Sliding Friction.*, Springer, New York, (1997).

(2) I.L. Singer and H.M. Pollock, *Fundamentals of Friction: Macroscopic and Microscopic Processes.* Dordrecht, Boston, (1992) p.299.

(3) M. Tomassone, J Sokoloff, A Widom, J Krim, Phys. Rev. Lett. **79**, 24, 4798, (1997).

(4) G.A Tomlinson, *A Molecular Theory of Friction*, Phil. Mag. **7**, 905-939 (1929).

(5) J.N. Israelachvili, D. Tabor, Proc. R. Soc. Lond. **A331**, 19 (1972).

(6) C.M. Mate, G.M. McClelland, R. Erlandsson, S. Chang, Phys. Rev. Lett. **59**, 1942 (1987).

(7) B.N.J. Persson and A. Nitzan, Surf. Sci. **367**, 261, (1996).

(8) B.N.J. Persson and A.I. Volokitin, Journal of Chem. Phys., **103**, 19, (1995).

(9) E. Smith and M. Robbins, Phys. Rev. B, **54**, 8252, (1996).

(10) C. Daly and J. Krim, Phys. Rev. Lett. **76**, 5, (1996).

(11) J.A. Venables, *Introducton to surface and Thin Film Processes*. Cambridge University Press, Cambridge, (2000) p.116.

(12) A. Thomy, Z. Duval, Surf. Sci. **299/300**, 415 (1994).

(13) J.G. Dash, *Between Two and Three Dimensions*. Physics Today. 26, (1985).

(14) J. Nakamura, H. Hirano, M Xie, I Matsuo, T. Yamada, K. Tanaka, Surf. Sci. **222**, L809 (1989).

(15) H.P. Bonzel and H.J. Krebs, Surf. Sci. **91**, 499, (1980).

(16) J. Nakamura and I. Toyoshima, Surf. Sci. **201**, 185, (1989).

(17) K.K. Kakati and H. Wilman, J. Phys.D: Apply Phys. **6**, 1307 (1973).

(18) Steven Winder. Ph.D. Dissertation, North Carolina State University, 2003.

(19) Omicron Nanotechnology, Multiprobe P with VT and AFT, www.omicron.de.

(20) V.V. Khvostov, V.G. Babaev, M.B. Guseva, Sov. Phys. Solid State **27(3)**, (1985).

(21) J. Krim and A. Widom, Phys. Rev. B, **38**, 12184 (1988).

(22) D. Salt, Hy-Q Handbook of Quartz Crystal Devices Van Nostrand Reinhold (UK) Co. Ltd., T.J. Press (Padstow) Ltd., Cornwall.

(23) Colorado Crystal Corporation, Part Number CCAT1BK-1004-000, (970) 667-9248.

(24) A. Widom and J. Krim, Phys. Rev. B, **34**, 1403 (1986).

(25) Crystek Crystals Corporation, Part Number CY7A, (800) 237-3061

(26) Tonya Coffey. Ph.D. Dissertation, North Carolina State University, 2004

(27) B. Borovsky and J. Krim, Journal of Applied Physics **88**, 7 (2000).

(28) C. Mak and J. Krim, Phys. Rev. B. **58**, 9 (1998).

(29) A.M. Shikin, G.V.Prudnikova, V.K. Adamchuk. Physical Review B, **62**, 19 (2000).